LE

NASA Technical Memorandum 87208

Variables Controlling Fatigue Crack Growth of Short Cracks

(NASA-TM-87208) VARIABLES CONTROLLING FATIGUE CRACK GROWTH OF SHORT CRACKS (NASA) 20 p HC A02/MF A01 CSCL 11F

N86-21661

Unclas

G3/26 05832

Jack Telesman and Douglas M. Fisher
Lewis Research Center
Cleveland, Ohio

and

Donna Holka
Michigan Technological University
Houghton, Michigan

Prepared for the
International Conference on Fatigue, Corrosion Cracking,
Fracture Mechanics, and Failure Analysis
sponsored by the American Society for Metals
Salt Lake City, Utah, December 2-6, 1985

NASA

VARIABLES CONTROLLING FATIGUE CRACK GROWTH OF SHORT CRACKS

Jack Telesman and Douglas M. Fisher
National Aeronautics and Space Administration
Lewis Research Center
Cleveland, Ohio 44135

and

Donna Holka
Michigan Technological University
Haughton, Michigan 49931

E-2865

SUMMARY

A study was conducted to evaluate the roles of crack closure and microstructure in the fatigue growth of short cracks. Testing was performed at R ratios of 0.1, 0.5, and 0.7. At all R ratios short cracks exhibited accelerated growth rates in comparison to long cracks. It was concluded that crack closure could not entirely account for the accelerated growth rates of short cracks. The accelerated growth rates occurred over crack lengths on the order of grain size, suggesting a strong influence of microstructure. A significant effect of grain boundaries and inclusions on short crack FCG behavior was observed. For very short crack lengths, fatigue growth rates do not appear to be a function of either ΔK or R ratio.

INTRODUCTION

Considerable effort has been made recently to explain the fatigue crack growth (FCG) behavior of short cracks. It has been recognized that short cracks exhibit accelerated growth rates which do not conform with predictions made on the basis of linear elastic fracture mechanics (LEFM) and long crack behavior.

A number of hypotheses have been postulated to account for the accelerated growth rate of short cracks. Among these, the crack closure hypothesis has gained considerable attention. This hypothesis, based on the difference in closure level between short and long cracks, was first proposed by Broek (ref. 1) and has been supported by others (refs. 2 to 5). The driving force for FCG is usually taken to be the applied stress intensity range (ΔK) with

$$\Delta K = K_{max} - K_{min} \tag{1}$$

where K_{max} and K_{min} are respectively the applied maximum and minimum stress intensities. However, Elber (ref. 6) noted that crack surfaces can be closed over a considerable portion of the load cycle. He proposed that the driving force for crack growth is an effective stress intensity (ΔK_{eff}) defined as

$$\Delta K_{eff} = K_{max} - K_{CL} \tag{2}$$

where K_{CL} is the highest stress intensity at which the crack tip is closed.

It has been hypothesized that closure stress increases with the increasing wake of the crack, and since short cracks have limited wakes, the amount of closure of these cracks is severely limited (refs. 2 to 5). Compared to large cracks, the lower closure level of small cracks results in a larger ΔK_{eff}. The larger ΔK_{eff} produces the more rapid FCG observed in small cracks.

Other investigators (refs. 7 to 9) have questioned the validity of the use of LEFM parameters to characterize short crack behavior. In the short crack regime localized plastic zone size can be on the order of the crack length, thus undermining one of the assumptions upon which LEFM parameters are based. Dowling (ref. 7) proposed the use of the elasto-plastic parameter ΔJ to characterize the short crack behavior. Lankford and Davidson (ref. 8) suggested that crack tip strains might successfully correlate short and long crack FCG data.

Since the short crack sizes can be comparable to the dimensions of microstructural features, it has been suggested that these features may play an important role in controlling short crack FCG behavior. For example it has been shown that short crack FCG rates slow down when approaching grain boundaries (ref. 10).

The purpose of this investigation was to evaluate some of the hypotheses that have been proposed to account for short crack behavior. To evaluate the closure hypothesis, short and long crack testing was performed at various R ratios (K_{max}/K_{min}) ranging from 0.1 to 0.7. The rationale was that at high enough R ratios the crack tip would be open during the entire loading cycle resulting in ΔK_{eff} to be equal to ΔK applied. In this case, according to the closure hypothesis, the FCG rates of both short and long cracks should be equal. Since the validity of the use of LEFM parameters to characterize short crack behavior has been questioned, an attempt was made to measure and correlate crack tip opening displacements (CTOD's) of the short cracks to their FCG rates. The benefit of using CTOD's to characterize short crack behavior, is that the CTOD is a measured variable directly related to the strain field at the crack tip. In addition, the effect of microstructural features such as grain boundaries, grain size and inclusions on short crack behavior was evaluated.

PROCEDURE

All long and short crack specimens, detailed in figure 1, were machined from a 3.2 mm (0.125 in.) thick sheet of 7075-T6 aluminum with tensile properties as detailed in table I. All specimen thicknesses were those of the as received sheet. The initial microstructure is shown in figure 2. For the long crack FCG studies compact tension (CT) specimens shown in figure 1(a), were used. The long crack tests were performed using a closed loop servohydraulic fatigue machine. The testing was done at R ratios of 0.1, 0.5, and 0.7 in an ambient air environment at 40 Hz. All testing and data acquisition was computer controlled using a compliance method to continuously monitor the crack length. The precracking of the CT specimens was performed with a following modified load shedding technique. By this technique specimens were initially subjected to stress intensity ranges large enough to initiate a crack. After a growth of 0.75 to 1.00 mm (0.030 to 0.040 in.), the stress intensity was decreased by 15 to 25 percent. This process was repeated until FCG rates of a

$2.5x10^{-10}$ m/c ($1x10^{-8}$ in./cycle) were achieved. The testing was restarted under a constant load amplitude at the final ΔK achieved during precracking. Only the data obtained during the increasing ΔK portion of the testing was used. Closure loads for the lower ΔK regime of the da/dN plot were measured for tests performed at R ratios of 0.1 and 0.7. The closure loads were determined from load displacement curves. The closure load was taken to be the first deviation from linearity during the unloading portion of the load displacement curve.

Short crack FCG tests were performed using a single edge notch (SEN) specimen detailed in figure 1(b). The edges of the notches were deburred. The notch surfaces were mechanically polished using polishing paper and diamond pastes. The final polishing with 0.5 μm diamond paste was in a tangential direction to the notch to prevent scratches in the thickness direction. Prior to testing, the notch surface was lightly etched using Kellers reagent to reveal the microstructure and remove any cold worked layers which may have resulted from polishing. Duplicate SEN specimens were tested using R ratios identical to those of the CT specimens. The loads used in the constant load amplitude tests are shown in table II. The short crack testing was performed at a frequency of 10 Hz (previous testing of this alloy in our laboratory showed the FCG rates to be independent of frequency in the range of 10 to 40 Hz). The crack length was monitored using a replication method. Acetate replicas were taken at 1000 cycle intervals. While taking replicas, the specimen was loaded to the maximum load so that CTOD could also be measured. The replicas were then coated with an approximately 400 Å sputtered Au alloy and photographed in a scanning electron microscope (SEM) to obtain crack length measurements. In order to avoid damage to the replicas from excessive heating, all the photomicrographs were obtained under a 10 kV applied potential. The stress intensity values were determined from a solution derived by Swain and Newman (ref. 11) for a semi-elliptical surface crack located at the center of a semi-circular notch.

RESULTS AND DISCUSSION

Long Cracks

The long crack FCG test results at R ratios of 0.1, 0.5, and 0.7 are shown in figure 3. All the data shown in this figure, including near threshold data, was obtained by performing constant load amplitude testing. This type of testing results in an increase in ΔK with an increase in crack length. It is more common to obtain near threshold regime data by performing a load shedding type of a test. However Newman (ref. 3) and James et al. (ref. 12) have shown recently that FCG data obtained by load shedding might be subject to increased crack closure effects. To avoid any such problems, only increasing ΔK testing was performed. The long crack data shown in figure 3 follows the typically observed trends. The FCG rates increase and the threshold stress intensity range decreases with an increase in the R ratio. A number of investigators (refs. 13 to 15) have suggested that the increase in FCG rates with an increase in the R ratio in the near threshold regime is due to the difference in crack closure for the various R ratios. Thus, if the FCG data was plotted versus ΔK_{eff}, all the data should collapse on one curve. Even though the evaluation of this hypothesis was not in the original scope of this work, the evaluation of the hypothesis was performed since the data was readily available. Crack closure readings were obtained for tests performed at R ratios of 0.1 and 0.7.

The measured K_{CL} readings are shown in table III. As seen there, for tests performed at an R ratio of 0.7 no crack closure was observed, indicating that the closure level was below that of the minimum applied stress intensity. Thus at an R of 0.7 the ΔK applied was always equal to ΔK_{eff}. A comparison of the FCG rates for the two R ratios in terms of both ΔK applied and ΔK_{eff} is shown in table IV. If the data is compared in terms of ΔK applied then there is a factor of two between the FCG rates at the two R ratios. However, there is an excellent agreement of the two FCG rates in terms of ΔK_{eff}. This result adds further support to the idea that the differences in FCG rates in the near threshold region are due to differences in crack closure.

Short Cracks

All the fatigue cracks observed in the SEN specimens initiated at brittle intermetallic inclusions. Examples of such initiation sites are shown in figure 4. The role of inclusions in crack initiation came into focus when a somewhat overetched specimen was tested. No crack initiation was observed in this specimen, even though the specimen was subjected to five times the number of fatigue cycles required to cause failure in a lightly etched specimen under similar loading conditions. Brittle intermetallic inclusions have been shown (ref. 16) to etch out preferentially with respect to other microstructural features, thus the absence of these inclusions resulted in a lack of initiation sites. Fatigue cracks as small as 5 to 10 μm in length (2(a) in fig. 1(b)), initiating from the above mentioned inclusions, could be resolved by the replication technique.

The measured short crack FCG rates at R ratios of 0.1, 0.5, and 0.7 are shown respectively in figures 5 to 7. For comparison purposes, the long crack data for the similar R ratio is also shown in each of these figures. A pronounced short crack behavior was observed at all R ratios evaluated. Thus short cracks were again found to propagate faster than long cracks at similar applied ΔK. Though no threshold stress intensities for the long cracks were measured, it is apparent from the data trends shown in figures 5 to 7 that the short cracks for all R ratios propagate at stress intensities below those of the threshold stress intensities of long cracks. It should be noted that the use of the replication technique allowed measurements of the FCG rates only in the through the thickness direction for the SEN specimen while the FCG rates of long cracks were obtained in the long transverse direction. However, Swain and Newman (ref. 11) using a similar specimen have shown that for another aluminum alloy the crack propagation rates in both directions were equivalent.

A considerable amount of data scatter was found to occur for some specimens, while others revealed considerably less. For comparison, results of the two R = 0.7 specimens tested under identical loading conditions are shown in figures 8(a) and 9(a). A number of factors were found to account for the data scatter. One factor is the jaggedness or tortuosity of the crack path. The respective crack paths of the two specimens showing different degrees of data scatter are shown in figures 8(b) and 9(b). The relatively straight crack path of the specimen shown in figure 8 resulted in little data scatter while the opposite is true for the jagged crack path specimen (fig. 9(b)). The stress intensity calculations used for data reduction were based only on a Mode I solution and no Mode II component of the stress intensity factor was taken into account. In addition, the crack length was measured as the projection of the

crack on to an imaginary plane perpendicular to the loading direction and not the actual distance the crack propagated. Obviously these two factors can influence the short crack FCG data.

Two microstructural features were found to influence the crack tortuosity. Crack growth direction often changed at grain boundaries as shown in figure 10. This behavior is probably due to the difference in crystallographic orientation of the two neighboring grains. Also cracks were found to change direction and preferentially follow brittle intermetallic inclusions. The observed process under which such crack deflection occurred consisted first of fracture of the intermetallic inclusion immediately ahead of the crack tip, followed by crack propagation toward the broken inclusion and finally by unification of the two cracks. An example of the process is shown in figure 11.

The results obtained in the study can be used to evaluate the closure hypothesis. As mentioned earlier, no crack closure was detected for the long crack specimen tested at R ratio of 0.7. Thus at this R ratio, the ΔK_{eff} is equal to the applied ΔK and the FCG rates of both the short and long cracks should be equal if differences in closure account entirely for the short crack behavior. However, as seen in figure 7, at this R ratio a pronounced short crack effect is present. This indicates that the difference in closure stress intensity between the long and short cracks is inadequate to explain short crack behavior. The data at a relatively high R ratio of 0.5 where closure effects are also probably minimal, shows the same trend and further corroborates the above conclusion.

A compilation of all the short crack data obtained in the present study reveals some interesting trends. As shown in figure 12, the data fits into two distinct regions marked in the figure by separate bands. The first band is of considerable interest since it contains the great majority of the data points exhibiting short crack behavior. It is interesting to note that in this band the average FCG rate remains constant as ΔK increases. Thus short crack FCG behavior appears not to be a function of either the stress intensity or the R ratio, in direct conflict with observed long crack behavior. This behavior suggests that ΔK might be an inappropriate parameter to correlate the growth of short cracks. The data points present in the second region represent somewhat longer crack lengths and they tend to follow established LEFM trends and correlate well with the long crack data base when the data in figures 3 and 12 are compared.

The approximate half-crack lengths (value of a in fig. 1(b)) at which short and long crack FCG rates converge were calculated for all R ratios and are shown in table V. For all R ratios evaluated, the crack lengths at which short and long crack data converged are approximately the same and are in the order of 30 to 40 μm. It should be pointed out that the above crack lengths include the width of the initial fractured inclusion (5 to 10 μm). Thus the pronounced short crack FCG behavior occurs during the first 20 to 35 μm of stable crack growth. It is very interesting to note that the grain size (i.e., thickness of the pancaked shaped grains) shown in figure 2, is in the order of 10 to 40 μm and thus approximately equal to the crack length under which short crack behavior occurs. This points to a possible strong influence of microstructure, and in particular grain size, on the behavior of short cracks. This conclusion is supported by the work of Lankford (ref. 17) and Brown et al. (ref. 18) who showed that the short crack behavior becomes more pronounced as grain sizes increases.

An attempt was made to correlate the short crack CTOD's with the short crack FCG data. Unfortunately, due to the tearing of the acetate tape on the edges of the open cracks, it was impossible to obtain reliable measurements of the CTOD's needed to make the correlation. Further efforts in this area are continuing.

CONCLUSIONS

1. At R ratios of 0.1, 0.5, and 0.7, short cracks propagated at higher FCG rates than long cracks at equivalent stress intensities. Also, at all R ratios, short cracks propagated at stress intensities below the threshold stress intensities of long cracks.

2. Differences in crack closure between short and long cracks could not account entirely for the accelerated FCG rates of short cracks.

3. In the region where short crack FCG rates were higher than those of long cracks, the FCG rates of short cracks appeared to be independent of the applied ΔK or the R ratio.

4. The half-crack lengths of short cracks at which short and long crack FCG rates converged were 30 to 40 μm. These crack lengths corresponded to the grain size of the alloy and suggest strong influence of microstructure on behavior of short cracks.

5. Due to experimental problems, it was not possible to correlate CTOD's to short crack FCG rates.

REFERENCES

1. Broek, D.: Elementary Engineering Fracture Mechanics, Noordhoff, p. 320.

2. Morris, W. L.; James, M. R.; Buck, O.: Growth Rate Models for Short Surface Cracks in AL-2219-T851. Met. Trans. A, Vol 12, No. 1, Jan. 1981, pp. 57-64.

3. Newman, Jr., J. C.: A Nonlinear Fracture Mechanics Approach to the Growth of Small Cracks Behavior of Short Cracks in Airframe Components, AGARD CP-328, 1982, pp. 6-1 to 6-26.

4. McGarver, J. F. and Ritchie R. O.; Fatigue Crack Propagation Thresholds for Long and Short Cracks in Rene 95 Nickel-base Superalloy. Matl. Science and Eng. Vol. 55, 1982, pp. 63-67.

5. Ritchie, R. O.; Suresh, S.: The Fracture Mechanics Similitude Concept: Questions Concerning Its Application to the Behavior of Short Fatigue Cracks. Matl. Science and Eng., Vol 57, 1983, pp. L27-L30.

6. Elber, W.: Fatigue Crack Closure Under Cyclic Tension. Eng. Frac. Mech., Vol. 2, No. 1, 1970, pp. 37-45.

7. Dowling, N. E.: Growth of Short Fatigue Cracks in an Alloy Steel. Scientific Paper 82-1D7-STINE-P1, Westinghouse R&D Center, 1982.

8. Lankford, J. and Davidson, D. L.: Near Threshold Crack Tip Strain and Crack Opening for Large and Small Fatigue Cracks. Proceedings Intern. Symp. on Fat. Crack Growth Threshold Conference, Davidson and Suresh, ed., AIME, 1984.

9. Leis, B. N: Displacement Controlled Fatigue Crack Growth in Inelastic Notch Fields: Implications for Short Cracks. Eng. Fracture Mech., Vol. 22, No. 2, 1985, pp. 279-293.

10. Brown, C. W. and Hicks, M. A.: A Study of Short Fatigue Crack Growth Behavior in Titanium Alloy, IM 685. Fat. of Eng. Matl. and Struct., Vol. 6, No. 1, 1983, pp. 67-76.

11. Swain, M. H. and Newman, J. C., Jr.: On the Use of Marker Loads and Replicas for Measuring Growth Rates for Small Cracks, AGARD-CP-376, AGARD, Nevilly-Sur-Seinne, France.

12. James, M. N. and Knott, J. F.: An Assessment of Crack Closure and the Extent of the Short Crack Regime in QIN (HY80) Steel. Fat. and Fract. of Eng. Matl. and Struct., Vol. 8, No. 2, pp. 177-191, 1985.

13. Venables, R. A., Hicks, M. A. and King, J. E.: Influence of Stress Ratio and Fatigue Thresholds and Structure Sensitive Crack Growth in Ni-Base Superalloys. Fatigue Crack Growth Threshold Concepts, ed. by Davidson and Suresh, AIME, 1984.

14. Blom, A. F.: Near Threshold Fatigue Crack Growth and Crack Closure in 17-4 PH steel and 2024-T3 Aluminum Alloy. Fatigue Crack Growth Concepts, ed. by Davidson and Suresh, AIME, 1984.

15. Beevers, C. J.; Bell, K. and Carlson, R. L.: Fatigue Crack Closure and Fatigue Threshold, ed., by Davidson and Suresh, AIME, 1984.

16. Lankford, J., Davidson, D. L. and Chan, K.S..: The Influence of Crack Tip Platicity in the Growth of Small Fatigue Cracks. Met. Trans. A, Vol. 15A, 1984, pp. 1579-1588.

17. Lankford, J.: The Growth of Small Fatigue Cracks in 7075-T6 Aluminum, Fat. of Eng. Matl. and Struct., Vol. 5, No. 3, 1982, pp. 233-248.

18. Brown, C. W.; King, J. E.; and Hicks, M. A.: Effects of Microstructure on Long and Short Crack Growth in Nickel Base Superalloys. Metal Science, Vol. 18, 1984, pp. 374-380.

TABLE I. - TENSILE PROPERTIES - 7075 - T6

Orientation	Ultimate strength		Yield strength		Elongation, percent
	MPa	ksi	MPa	ksi	
Longitudinal	565	82	524	76	12
Long transverse	579	84	517	75	13

TABLE II. - LOADS USED IN SHORT CRACK TESTING

R	Max load		Min load	
	N	lb	N	lb
0.1	22 240	5 000	2 224	500
0.5	35 584	8 000	17 920	4 000
0.7	53 376	12 000	37 363	8 400

TABLE III. - CRACK CLOSURE STRESS INTENSITIES OF LONG CRACKS

R = 0.1		R = 0.7	
ΔK Applied MPa$\sqrt{m}$, ksi$\sqrt{in.}$	K_{CL} MPa$\sqrt{m}$, ksi$\sqrt{in.}$	ΔK Applied MPa$\sqrt{m}$, ksi$\sqrt{in.}$	K_{CL} MPa$\sqrt{m}$, ksi$\sqrt{in.}$
1.65 (1.5)	(b)	1.65 (1.5)	(a)
3.14 (2.85)	1.15 (1.04)	3.14 (2.85)	(a)
4.4 (4.0)	1.28 (1.16)	4.4 (4.0)	(a)
4.95 (4.5)	1.29 (1.17)	4.95 (4.5)	(a)
5.61 (5.1)	1.30 (1.18)	5.61 (5.1)	(a)

[a]$K_{CL} < K_{min}$, no actual value of K_{CL} was determined since it would have required applying loads below K_{min} which are known to affect subsequent FCG rates.
[b]Not measured.

TABLE IV. - COMPARISON OF FCG RATES IN TERMS OF APPLIED ΔK and ΔK_{eff}

R	K_{max} MPa$\sqrt{m}$, ksi$\sqrt{in.}$	K_{min} MPa$\sqrt{m}$, ksi$\sqrt{in.}$	K_{CL} MPa$\sqrt{m}$, ksi$\sqrt{in.}$	ΔK Applied MPa$\sqrt{m}$, ksi$\sqrt{in.}$	ΔK_{eff} MPa$\sqrt{m}$, ksi$\sqrt{in.}$	da/dN m/cycle, in./cycle
0.1	3.49 (3.17)	0.35 (0.32)	1.15 (1.04)	3.14 (2.85)	2.34 (2.13)	3.1×10^{-9} (1.2×10^{-7})
0.7	7.8 (7.09)	5.46 (4.96)	(a)	2.34 (2.13)	2.34 (2.13)	3×10^{-9} (1.2×10^{-7})
0.7	10.47 9.52	7.33 (6.66)	(a)	3.14 (2.85)	3.14 (2.85)	6×10^{-9} (2.4×10^{-7})

[a]$K_{CL} < K_{min}$

TABLE V. - APPROXIMATE HALF-CRACK LENGTHS OF SHORT CRACKS AT CONVERGENCE OF FCG RATES

R	Crack length (a) μm, (in.)
0.1	37 (0.0015)
0.5	30 (0.0012)
0.7	37 (0.0015)

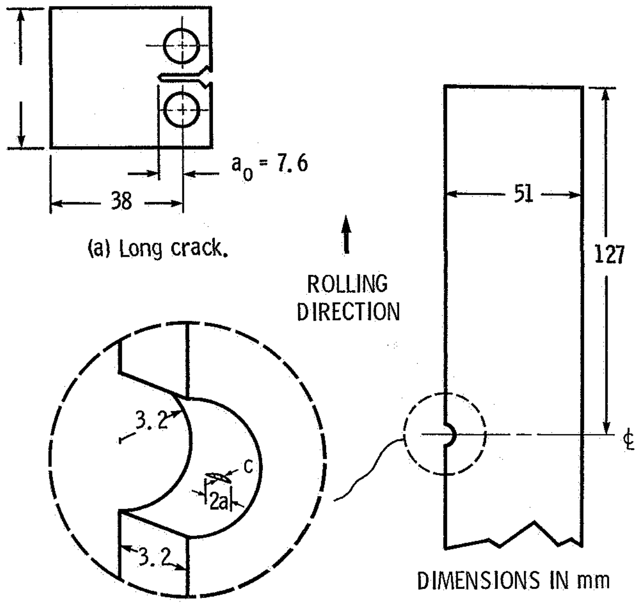

(b) Short crack.

Figure 1. - Test specimens.

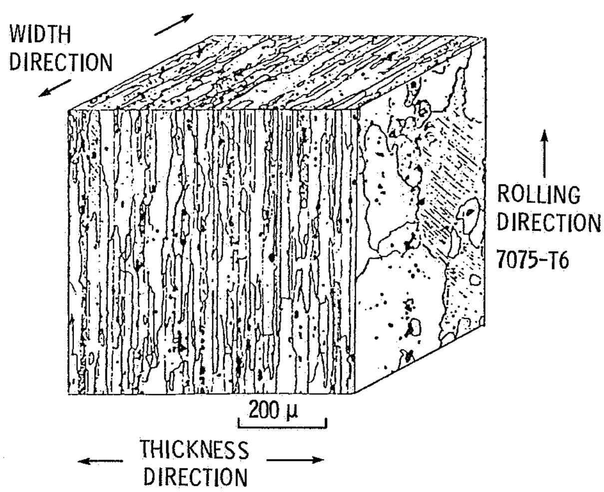

Figure 2. - 7075-T6 Microstructure.

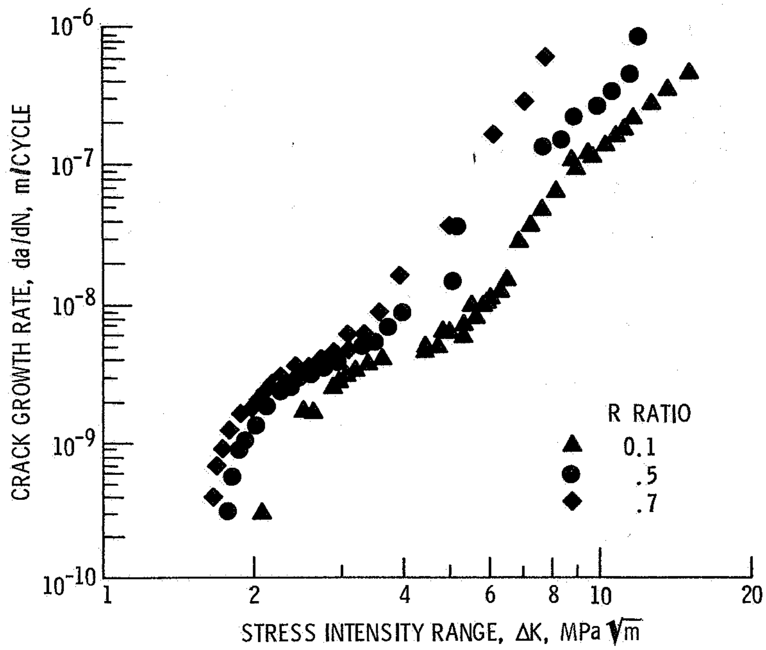

Figure 3. - Long crack test results.

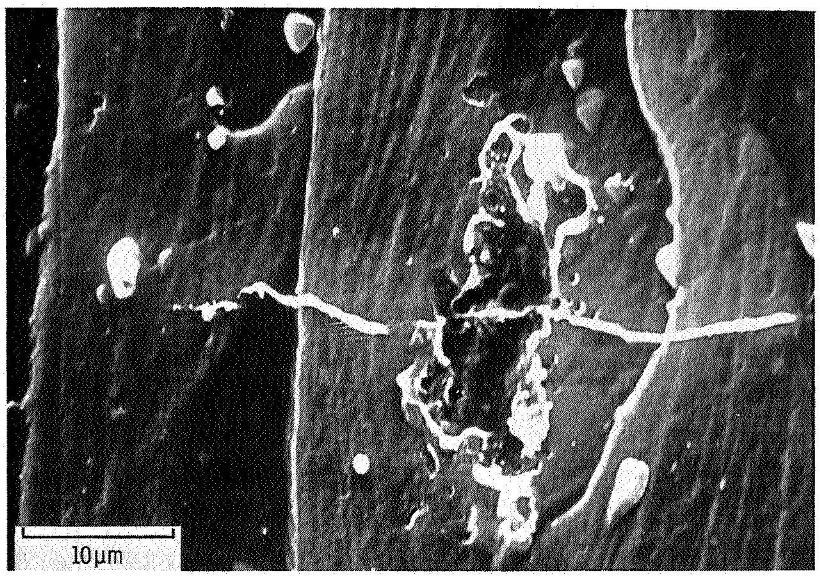

(a) Notch surface.

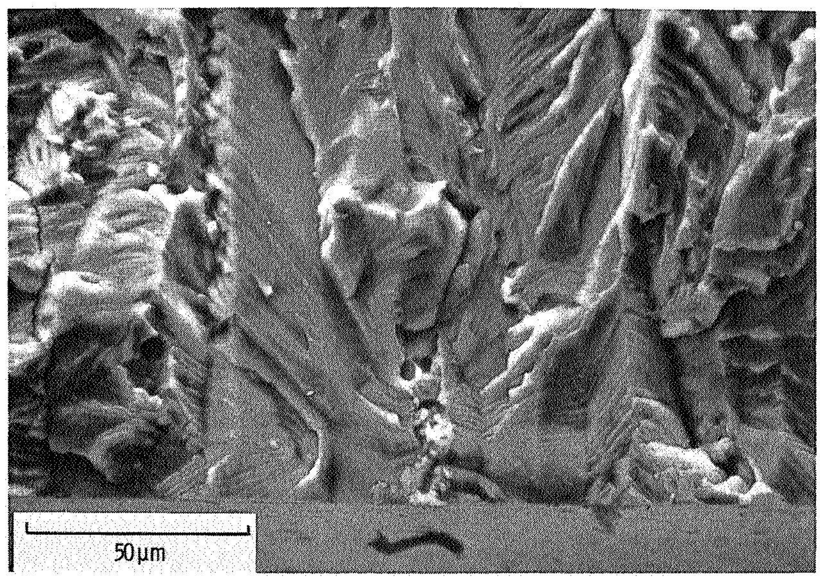

(b) Fracture surface.

Figure 4. - Examples of crack initiation at inclusions.

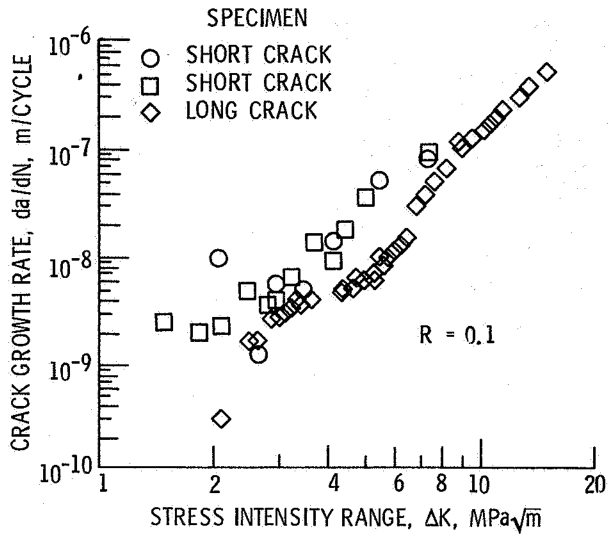

Figure 5. - Short and long crack growth rates at R ratio of 0.1.

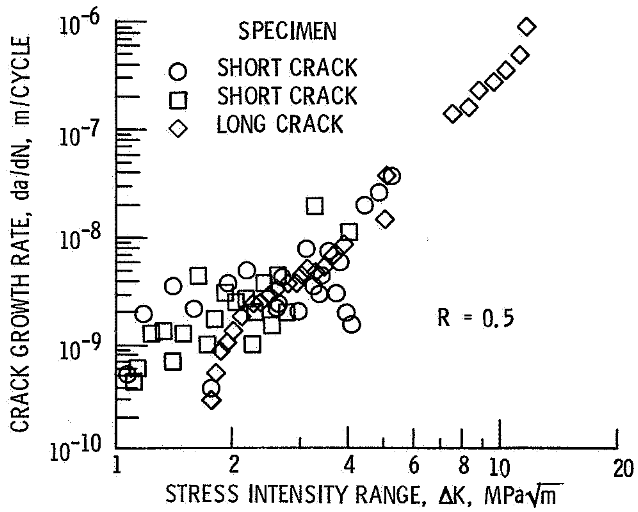

Figure 6. - Short and long crack growth rates at R ratio of 0.5.

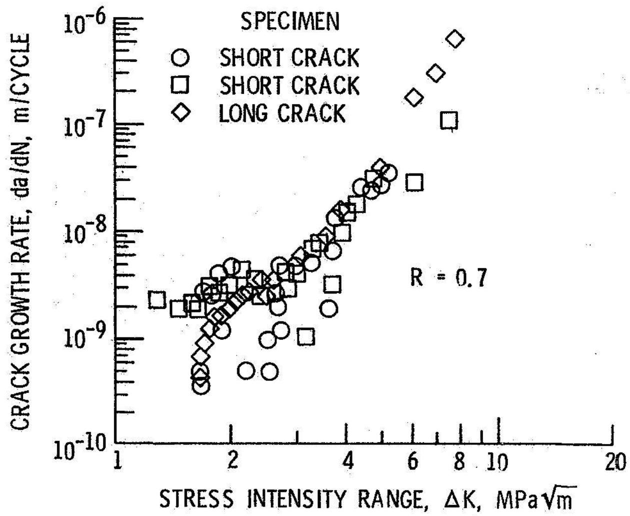

Figure 7. - Short and long crack growth rates at R ratio of 0.7.

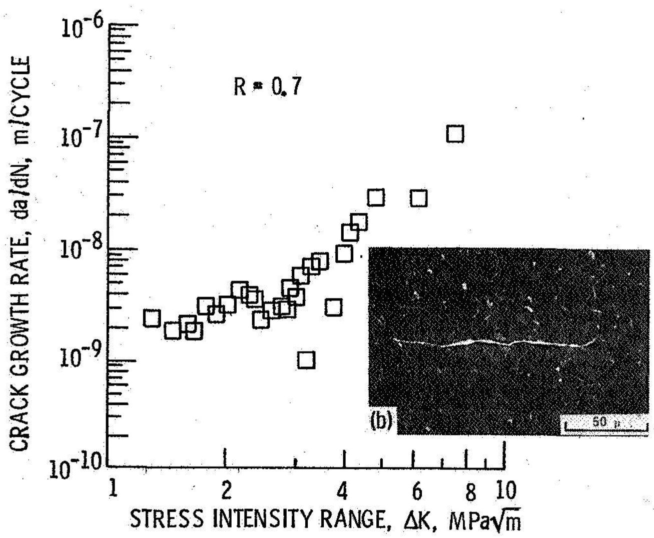

Figure 8. - Growth rates associated with a straight short crack profile.

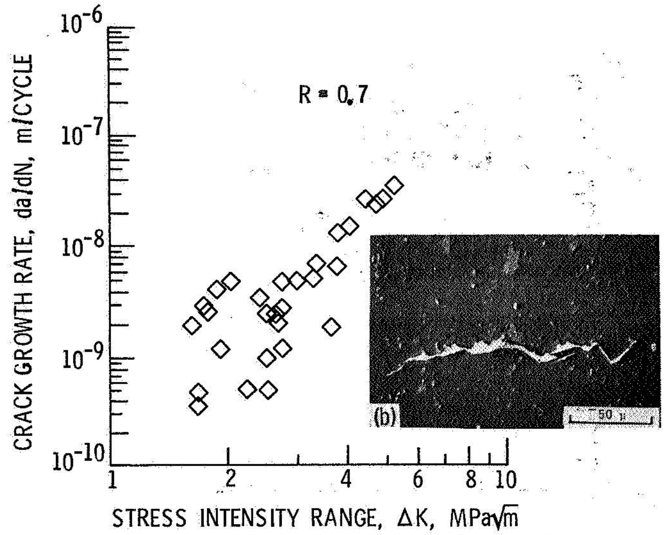

Figure 9. - Growth rates associated with a jagged short crack profile.

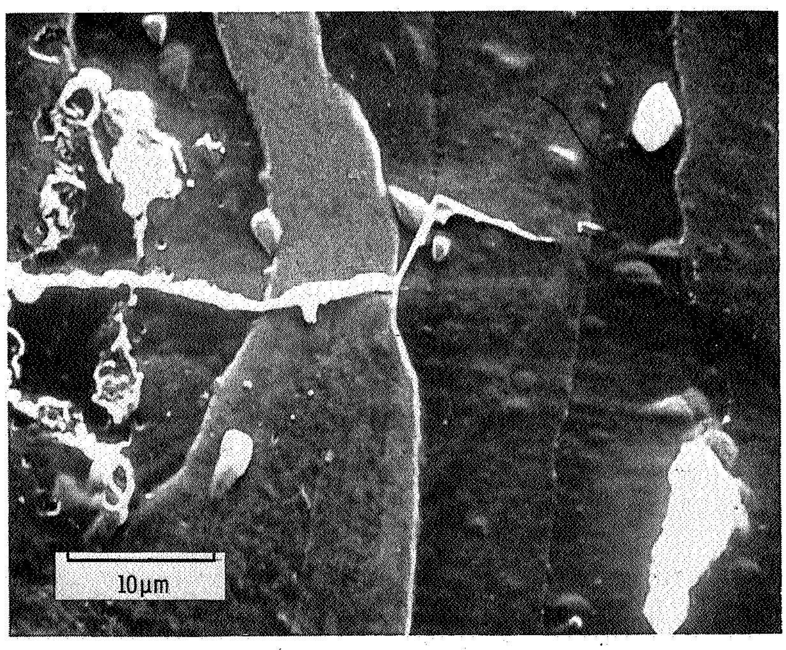

Figure 10. - Influence of grain boundaries on the crack path.

ORIGINAL PAGE IS
OF POOR QUALITY

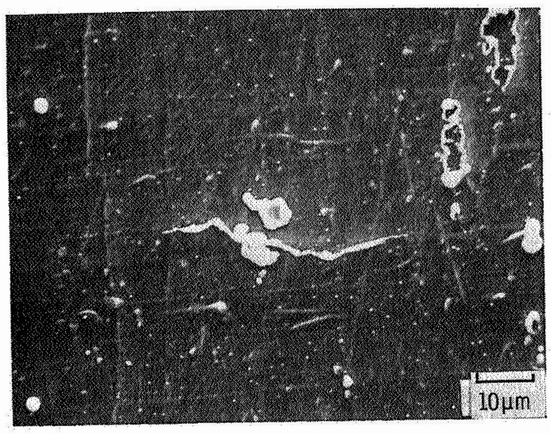

(a) 13 000 cycles.

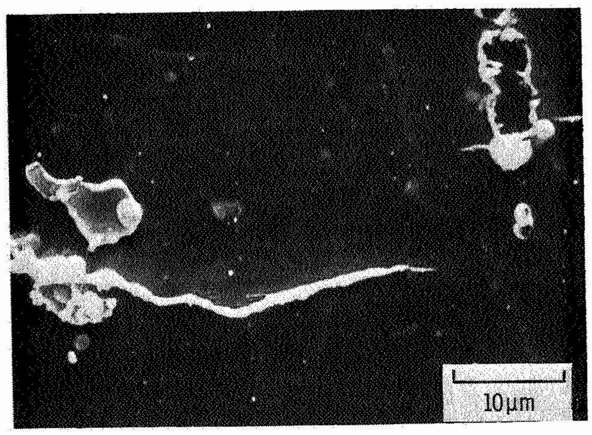

(b) 14 000 cycles.

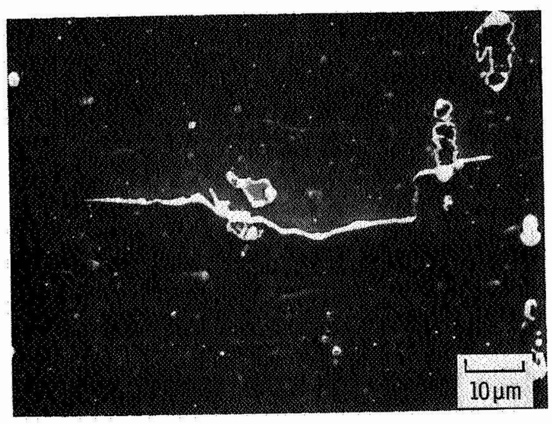

(c) 15 500 cycles.

Figure 11. - Influence on crack path by inclusions ahead of crack tip.

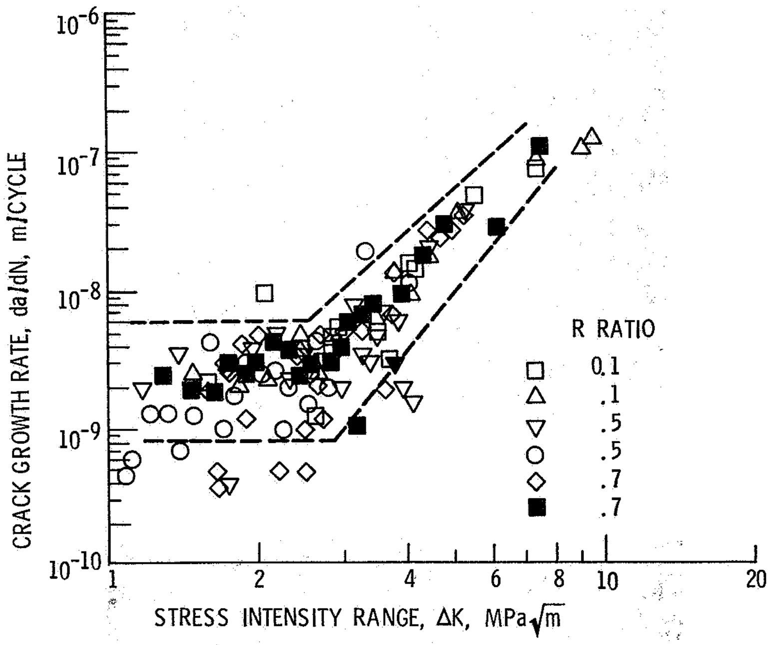

Figure 12. - Compilation of all short crack results.

1. Report No.	2. Government Accession No.	3. Recipient's Catalog No.
NASA TM-87208		

4. Title and Subtitle	5. Report Date
Variables Controlling Fatigue Crack Growth of Short Cracks	
	6. Performing Organization Code 505-33-7C
7. Author(s) Jack Telesman, Douglas M. Fisher, and Donna Holka	8. Performing Organization Report No. E-2865
	10. Work Unit No.
9. Performing Organization Name and Address National Aeronautics and Space Administration Lewis Research Center Cleveland, Ohio 44135	11. Contract or Grant No.
	13. Type of Report and Period Covered Technical Memorandum
12. Sponsoring Agency Name and Address National Aeronautics and Space Administration Washington, D.C. 20546	14. Sponsoring Agency Code

15. Supplementary Notes

Jack Telesman and Douglas M. Fisher, NASA Lewis Research Center; Donna Holka, Michigan Technological University, Houghton, Michigan 49931. Prepared for the International Conference on Fatigue, Corrosion Cracking, Fracture Mechanics, and Failure Analysis, sponsored by the American Society for Metals, Salt Lake City, Utah, December 2-6, 1985.

16. Abstract

A study was conducted to evaluate the roles of crack closure and microstructure in the fatigue growth of short cracks. Testing was performed at R ratios of 0.1, 0.5, and 0.7. At all R ratios short cracks exhibited accelerated growth rates in comparison to long cracks. It was concluded that crack closure could not entirely account for the accelerated growth rates of short cracks. The accelerated growth rates occurred over crack lengths on the order of grain size, suggesting a strong influence of microstructure. A significant effect of grain boundaries and inclusions on short crack FCG behavior was observed. For very short crack lengths, fatigue growth rates do not appear to be a function of either ΔK or R ratio.

17. Key Words (Suggested by Author(s))	18. Distribution Statement
Crack closure Fatigue crack propagation Short cracks	Unclassified - unlimited STAR Category 26

19. Security Classif. (of this report)	20. Security Classif. (of this page)	21. No. of pages	22. Price*
Unclassified	Unclassified		

*For sale by the National Technical Information Service, Springfield, Virginia 22161